Article

Superhydrophobic, Superoleophobic and Antimicrobial Coatings for the Protection of Silk Textiles

Dimitra Aslanidou and Ioannis Karapanagiotis * (iD)

Department of Management and Conservation of Ecclesiastical Cultural Heritage Objects,
University Ecclesiastical Academy of Thessaloniki, 54250 Thessaloniki, Greece; aslanidou.dimitra@gmail.com
* Correspondence: y.karapanagiotis@aeath.gr; Tel.: +30-2310-301784

Abstract: A method to produce multifunctional coatings for the protection of silk is developed. Aqueous dispersion, free of any organic solvent, containing alkoxy silanes, organic fluoropolymer, silane quaternary ammonium salt, and silica nanoparticles (7 nm in mean diameter) is sprayed onto silk which obtains (i) superhydrophobic and superoleophobic properties, as evidenced by the high contact angles (>150°) of water and oil drops and (ii) antimicrobial properties. Potato dextrose agar is used as culture medium for the growth of microorganisms. The protective coating hinders the microbial growth on coated silk which remains almost free of contamination after extensive exposure to the microorganisms. Furthermore, the multifunctional coating induces a moderate reduction in vapor permeability of the treated silk, it shows very good durability against abrasion and has a minor visual effect on the aesthetic appearance of silk. The distinctive roles of the silica nanoparticles and the antimicrobial agent on the aforementioned properties of the coating are investigated. Silica nanoparticles induce surface structures at the micro/nano-meter scale and are therefore responsible for the achieved extreme wetting properties that promote the antimicrobial activity. The latter is further enhanced by adding the silane quaternary ammonium salt in the composition of the protective coating.

Keywords: superhydrophobic; superoleophobic; antimicrobial; siloxane; nanoparticle; silk; textile; abrasion; color

1. Introduction

Superhydrophobic, superoleophobic, and other surfaces of extreme wetting properties have attracted the interest of many researchers owing to their wide range of potential applications [1,2]. Superhydrophobicity is usually achieved by developing a special hierarchical micrometer and nanometer sized structure [3] on the surface of interest and applying low surface energy agents [4]. Within the last two decades, specialized set-ups have been developed to control micro/nano-scale surface structures, leading to the fabrication of superhydrophobic surfaces [3–13]. Among the most common methods are lithographic patterning [14,15], sol gel [16,17], layer by layer deposition [18], chemical vapor deposition [19], plasma etching [20], and nanoparticle deposition [13,21–26]. Similar strategies, such as plasma treatment, self-assembly, electrochemical deposition, magnetron sputtering deposition, chemical vapor deposition, and polymer-nanoparticle coatings, have been adopted to produce superoleophobic and superomniphobic surfaces [27–41]. These are surfaces that have the ability to repel liquids with surface tensions lower than that of water (=72 mN/m).

Superhydrophobicity and superoleophobicity can have an enormous impact on the textile industry. Hence, the attention of several researchers has focused on the development of methods that induce extreme wetting properties in textiles. Hoefnagels et al. deposited nanoparticles on cotton fibers to

generate a dual-size surface roughness, while superhydrophobization was achieved using PDMS [42]. Artusa et al. [43] fabricated a superoleophobic polyester fabric coated with silicone nanofilaments, followed by plasma fluorination. Leng at al. [44] deposited charged micro- and nano-particles on cotton thus inducing a hierarchical structure. After the application of a perfluorodecyltrichlorosilane, the treated cotton obtained superhydrophobic properties [44]. Liu et al. [45] produced superhydrophobic cotton using silica nanoparticles and octadecyltrichlorosilane, as a low surface energy agent. Furthermore, superhydrophobic/superoleophobic textiles have been fabricated via layer by layer assembly [46], sol-gel [47], chemical vapor phase deposition [48], and other methods [49–51].

The textile industry has a strong interest in the production of fabrics with antimicrobial properties [52–55]. Combining the special wetting (superhydrophobic, superoleophobic) and antimicrobial properties in a single coating product can open new avenues for the textile industry [56–65]. We have recently developed a method to produce superhydrophobic and superoleophobic coatings on silk textiles [66]. In the present work, we induce another useful property to the protective coating: the antimicrobial resistance. Therefore, a multifunctional coating is produced for the protection of silk that obtains superhydrophobic, superoleophobic, and antimicrobial properties. The coating is prepared using an aqueous dispersion of alkoxy silanes, an organic fluoropolymer, a silane quaternary ammonium salt, and silica nanoparticles. The multifunctional coating induces a moderate reduction in vapor permeability of the treated silk, shows very good durability against mechanical abrasion and has a minor visual effect on the aesthetic appearance of silk.

2. Materials and Methods

2.1. Production and Surface Characterization of Coated Silk Samples

Coatings were produced using (i) a water-soluble emulsion of alkoxy silanes and organic fluoropolymer (Silres BS29A, Wacker, Munich, Germany), (ii) a silane quaternary ammonium salt, (AEM 5700, Aegis, Midland, MI, USA) which is an antimicrobial product of 3-(trimethoxysilyl) propyldimethyloctadecyl ammonium chloride and (iii) silica (SiO_2) nanoparticles of 7 nm in mean diameter (Sigma-Aldrich, St. Louis, MO, USA). No organic solvents were used in the study. Two aqueous emulsions of 7% *w/w* Silres BS29A and 7% *w/w* Silres BS29A with 1% *w/w* silane quaternary ammonium salt were prepared, designated as Siloxane and Siloxane+AM hereafter, respectively. Silica nanoparticles were dispersed in the two aforementioned emulsions at a concentration of 1% *w/w*, resulting in two dispersions, designated as Siloxane+SiO_2 and Siloxane+AM+SiO_2. The concentrations for the siloxane material and the SiO_2 nanoparticles were selected according to the results of a previous report [66], whereas the concentration of the AM material was selected following the recommendations of the manufacturer (Aegis).

Emulsions and dispersions were stirred vigorously for 30 min and sprayed onto clean 4 cm × 5 cm silk specimens, purchased from the local market. An airbrush system (Paasche Airbrush, Chicago, IL, USA) with a nozzle of 660 μm diameter was used for the deposition of the emulsions and dispersions. Each coating was produced by depositing 1 mL of the emulsion/dispersion while the airbrush was held at a distance of 20 cm from the silk surface. Treated silk specimens were annealed at 40 °C overnight to remove residual solvent (water) and kept at room temperature for 2–3 days. In summary, four types of silk specimens were produced coated by Siloxane, Siloxane+AM, Siloxane+SiO_2, and Siloxane+AM+SiO_2.

Scanning Electron Microscopy equipped with an Energy Dispersive X-ray Spectrometer (SEM-EDX; JEOL, JSM-6510 & Oxford, Tokyo, Japan & Abingdon, UK) was used for elemental analyses of the coated specimens and to study their surface structures. Prior to the SEM-EDX and SEM studies, the specimens were coated with a thin layer of carbon.

Drops (8 μL) of distilled water and olive oil (purchased from local market) were placed onto coated silk samples, and the contact angles were measured using an optical tensiometer apparatus (Attension Theta, Gothenburg, Sweden). The reported contact angles are averages of five measurements. Contact

angles of water and oil drops on bare silk could not be experimentally measured as both liquids were quickly absorbed by the uncoated reference silk.

2.2. Evaluation of the Antimicrobial Properties of Treated Silk

The experimental protocol for the evaluation of the antimicrobial activities of the produced coatings was adopted from a previously published study [67]. An aqueous solution of potato dextrose agar (Sigma-Aldrich, St. Louis, MO, USA) was prepared (39 g/L) and heated to a boil. Agar was then poured onto a sterile petri dish. Once the agar was solidified, microorganisms were left to culture on deteriorated strawberries that were transferred on the agar with an inoculation loop. The silk sample was positioned on the plastic support and the petri dish was hermetically closed. The petri dish was then placed in an incubator at 37 °C for 144 h. The contaminated silk sample was then removed from the agar and left to dry. Uncoated reference silk and silk samples coated by Siloxane, Siloxane+AM, Siloxane+SiO$_2$, and Siloxane+AM+SiO$_2$ were treated. The evolution of the microbial growth was ascertained by a Leica microscope, model MZ125 (Wetzlar, Germany) and a Zeiss Axioskop 40 (Jena, Germany) polarizing light microscope.

Digital photographs were manipulated by the thermal imaging effect and treated with image J. software. By changing the threshold color, we defined the highly contaminated and the non-contaminated regions. Measurement of the area that each region occupied on the coated silk samples, offered an indirect quantification of the antimicrobial efficiencies of the protective coatings. The results are described in the Supplementary File.

For the absorption measurements, the samples were placed inside test tubes with 15 mL of sterile potato dextrose agar (19.5 g/L) and vortex agitation was introduced in order to help the release of the microorganisms from the silk surfaces into the agar medium. The absorption of the agar solution was measured and compared to that of a sterile agar solution in the UV-Vis. The turbidity of the solution increases as the growth of microorganisms is higher [67]. Thus, the absorption measurement becomes an index that shows the effectiveness of the applied coating. Absorption measurements were conducted in the range of 200–1200 nm using a spectrophotometer UV1800 (Shimadzu, Kyoto, Japan). The results are described in the Supplementary File.

2.3. Other Evaluation Tests

The water vapor permeability was conducted according to the standard test method ASTM E96/E9610. Uncoated and coated silk specimens were used to seal glass vessels filled with water and were placed in a chamber at 30 °C. The weight losses of the vessels were measured every 24 h. The total duration of the test was 120 h, and five measurements were taken for each sample. Abrasion resistance was evaluated according to the standard test method ASTM D3884-09 using a Taber Industries Abrasion Tester-Model 5135 (North Tonawanda, NY, USA). Measurements were conducted in triplicate. Finally, colorimetric measurements were carried out using a Miniscan XE Plus spectrophotometer from HunterLab (Reston, VA, USA) and the results were evaluated using the *L* a* b** coordinates of the CIE 1976 scale. The reported results are averages of three measurements.

3. Results and Discussion

3.1. SEM-EDX Characterization

Figure 1a,b show the results of the SEM-EDX analyses of silk samples coated by Siloxane and Siloxane+AM, respectively. The detections of Si and F in the spectra of both Figure 1a,b are attributed to the siloxane and fluoropolymer, respectively, which are contained in the Siloxane product (Silres BS29A). Cl recorded only in the spectrum of Figure 1b originates from the antimicrobial agent, and it is therefore not detected in Figure 1a. Other elements included in the spectra of Figure 1 such as O, S, and Ca were also detected in uncoated silk (not shown). Overall, the results of the SEM-EDX study are in agreement with the chemical compositions provided by the manufacturers of the Siloxane and AM

products. Moreover, the SEM-EDX results confirm that the coatings were successfully deposited onto the silk samples.
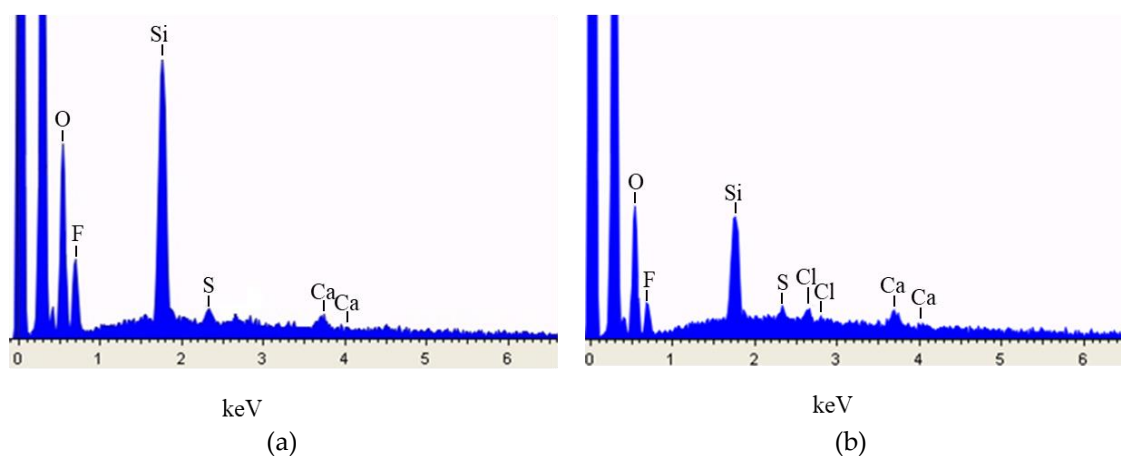
Figure 1. Scanning Electron Microscopy equipped with an Energy Dispersive X-ray Spectrometer (SEM-EDX) spectra of silk samples coated by (**a**) Siloxane and (**b**) Siloxane+AM.

3.2. Wetting Properties and Surface Structures

The results of the contact angle (CA) measurements are reported in Table 1. The CA of water drops on Siloxane on silk is 148.7° and decreases to 143.0° when AM is added to the protective coating (Siloxane+AM). This may be considered as a slight decrease taking into account the variations in the CA measurements which are included in Table 1. The use of the SiO_2 nanoparticles has a major impact on the wetting properties of the coatings. In particular, adding SiO_2 to the Siloxane matrix results in an increase of the CA of water drops from 148.7° (Siloxane) to 164.3° (Siloxane+SiO_2), whereas adding SiO_2 to the Siloxane+AM coating results in an increase of the CA from 143.0° (Siloxane+AM) to 155.3° (Siloxane+AM+SiO_2). Consequently, superhydrophobicity is achieved in both coatings, which are enriched with SiO_2 nanoparticles. Interestingly, lower CA of water drops was measured on Siloxane+AM+SiO_2 than on Siloxane+SiO_2, implying that the AM agent has a negative effect on hydrophobicity. A similar decrease, which was much smaller in magnitude, was recorded between the Siloxane and the Siloxane+AM coatings, as discussed above.

Table 1. Contact angle (CA) measurements (°) of water and oil drops on coated silk.

| Drop	CA (°) on Coated Silk			
	Siloxane	**Siloxane+AM**	**Siloxane+SiO$_2$**	**Siloxane+AM+SiO$_2$**
Water	148.7 ± 2.8	143.0 ± 2.5	164.3 ± 3.3	155.3 ± 2.7
Oil	138.4 ± 4.8	141.4 ± 2.1	147.6 ± 5.9	157.0 ± 3.3

According to the results of Table 1, the use of the SiO_2 nanoparticles has a major impact on the CA of oil drops. In particular, adding SiO_2 to the Siloxane coating results in an increase of CA of oil drops from 138.4° (Siloxane) to 147.6° (Siloxane+SiO_2), whereas adding SiO_2 to the Siloxane+AM coating results in an increase of the CA from 141.4° (Siloxane+AM) to 157.0° (Siloxane+AM+SiO_2). Consequently, superoleophobicity is almost and clearly achieved on the Siloxane+SiO_2 and Siloxane+AM+SiO_2 coatings, respectively. Interestingly, adding the AM agent to the Siloxane+SiO_2 coating clearly has a positive impact on the CA of oil drops, which increases from 147.6° (Siloxane+SiO_2) to 157.0° (Siloxane+AM+SiO_2). Without the presence of the SiO_2, however, the effect of the AM is negligible as the CA of oil drops increases from 138.4° (Siloxane) to only 141.4° (Siloxane+AM), which is a difference within the given experimental variations.

Overall, the results of Table 1 suggest that the SiO_2 nanoparticles promote the extreme wetting properties enhancing both the hydrophobic and oleophobic characters of the coatings. The effect of the AM agent on the wetting properties is more complex. The use of the AM agent into the Siloxane+SiO_2 composition enhances the oleophobic character of the coating while at the same time it has a negative effect on the hydrophobic character of the coating. Without the presence of the SiO_2 nanoparticles, however, the effect of the AM on the wetting properties of the coatings is negligible, as comparable CA of water and oil drops were measured on Siloxane and Siloxane+AM coatings on silk.

The surface structures of the four coatings included in Table 1 are revealed in the SEM images of Figure 2. When silk is covered with Siloxane, there is no significant surface structure originated by the deposited coating (Figure 2a). Likewise, the AM agent does not induce any significant change on the surface structure (Figure 1b). However, a careful comparison of the SEM images in Figure 1a (Siloxane) and 1b (Siloxane+AM) can support a slight increase in surface roughness induced by the presence of the AM product. According to the literature, the quaternary ammonium salt is covalently bound to the silk fibers [68,69]. Although the exact antimicrobial mechanism has not been fully elucidated, it is mainly attributed to a mechanical disruption of the microorganisms' cell membrane, which should lead to increased surface roughness [70–72].
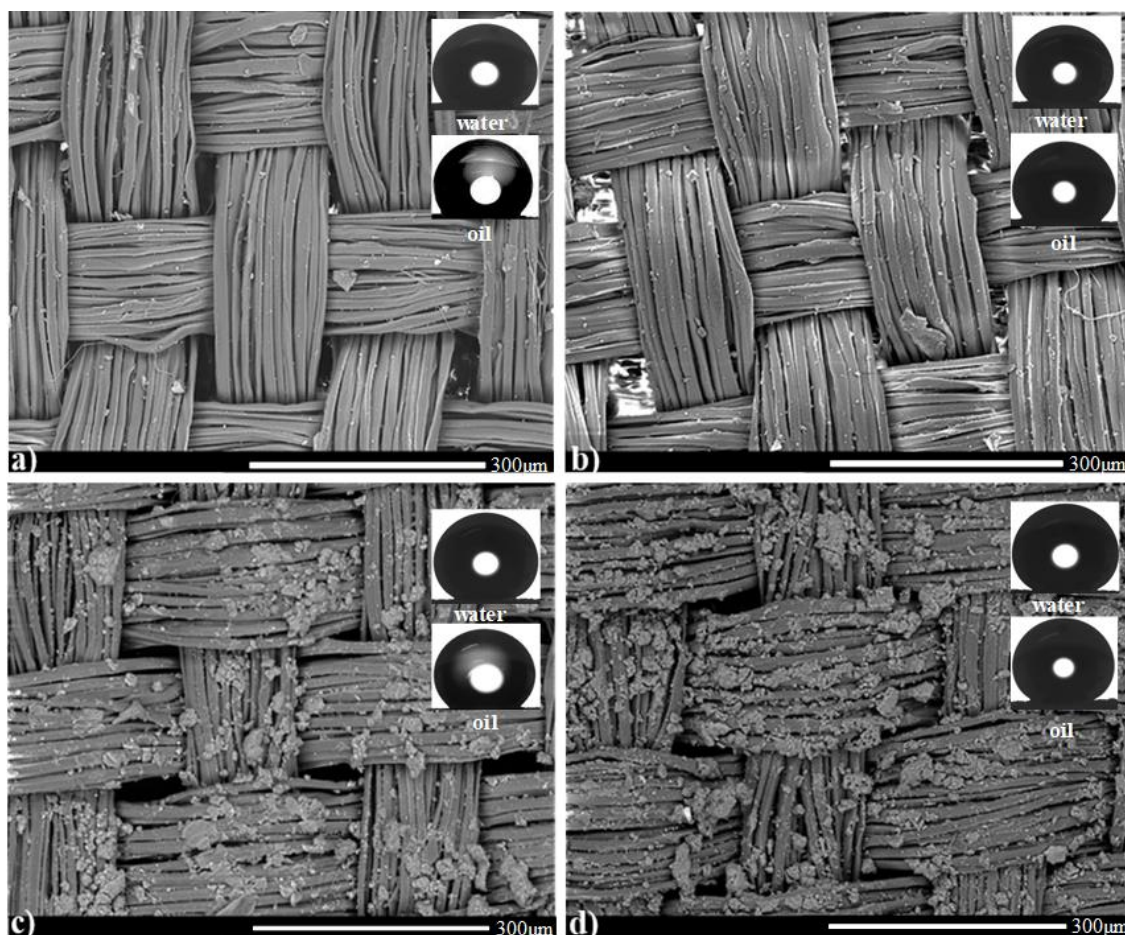

Figure 2. SEM images of silk coated by (**a**) Siloxane, (**b**) Siloxane+AM, (**c**) Siloxane+SiO_2, and (**d**) Siloxane+AM+SiO_2. Photographs of water and oil drops on the coated silk samples are included.

As shown in the SEM image of Figure 2c, adding SiO_2 nanoparticles in the Siloxane coating results in the formation of microscale clusters with nanostructures, which in turn induce an augmented surface roughness at the micrometer and nanometer scale. The enhanced roughness leads to the high values of the CA of water and oil drops on the Siloxane+SiO_2 coatings, as reported in Table 1.

This dramatic effect of nanoparticles-additives in the surface structures of polymer+nanoparticles coatings has been discussed in several previously published reports [8,13,21–24,66]. As revealed by the SEM image of Figure 2d, the surface roughness increases further by adding the AM agent into the Siloxane+SiO$_2$ composition. The surface structure in Figure 2d is denser compared to the image of the specimen that does not contain the AM component (Figure 2c). This highly rough structure enhances the oleophobic character of the coating, implying that higher CA of oil drops should be measured on Siloxane+AM+SiO$_2$ than on Siloxane+SiO$_2$ coatings, as reported in Table 1. In principle, the same behavior should be expected for the CA of water drops. However, the results of the CA of water drops in Table 1 show otherwise: adding AM to the composite Siloxane+SiO$_2$ coating results in lower CA. We suggest that this effect can be raised by the inherent hydrophilic nature of the AM agent. Therefore, when the hydrophilic AM material is added to the composition of the protective coating (Siloxane+AM+SiO$_2$), two opposing effects are induced: surface roughness increases and this tends to enhance hydrophobicity (and oleophobicity), but an inherent hydrophilic material is added, and this tends to diminish the hydrophobic character of the surface of the coating. The latter effect is dominant, according to the results of Table 1, which show that the CA of water drops is lower on Siloxane+AM+SiO$_2$ than on Siloxane+SiO$_2$ coatings.

3.3. Antimicrobial Activity

Photographs demonstrating the cultivation process and development of the microorganisms on silk samples are provided in Figure 3 as examples. Figure 4 shows the responses of the uncoated (Figure 4a) and coated silk samples (Figure 4b–e) to the evolution of the microorganism population.
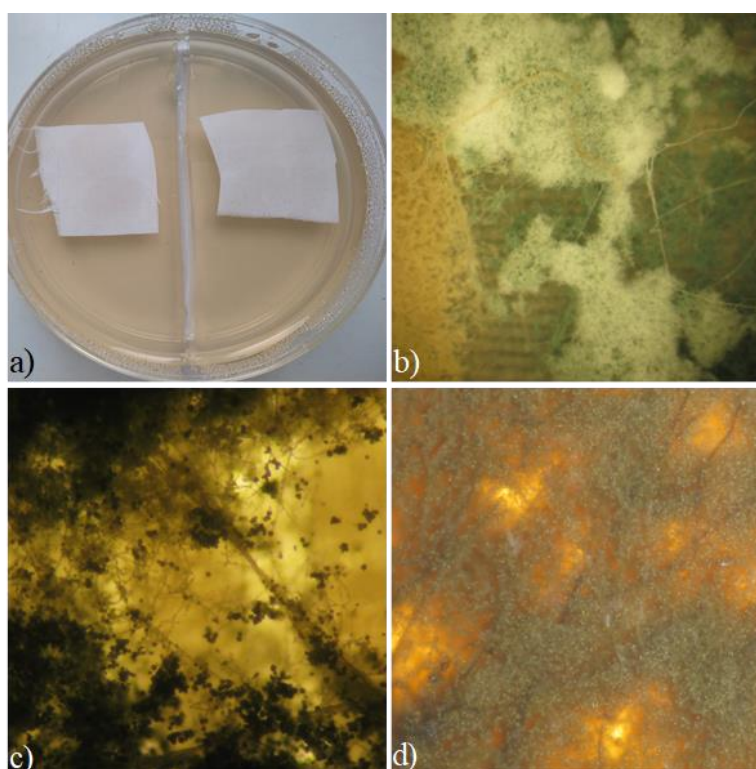
Figure 3. (**a**) Silk samples coated by Siloxane+SiO$_2$ (left) and Siloxane+AM+SiO$_2$ (right) are positioned on the petri dish prior to culture. Indicative microphotographs showing the development of microorganisms on silk coated by Siloxane are shown under magnifications 50× in (**b**) and 320× in (**c**,**d**).
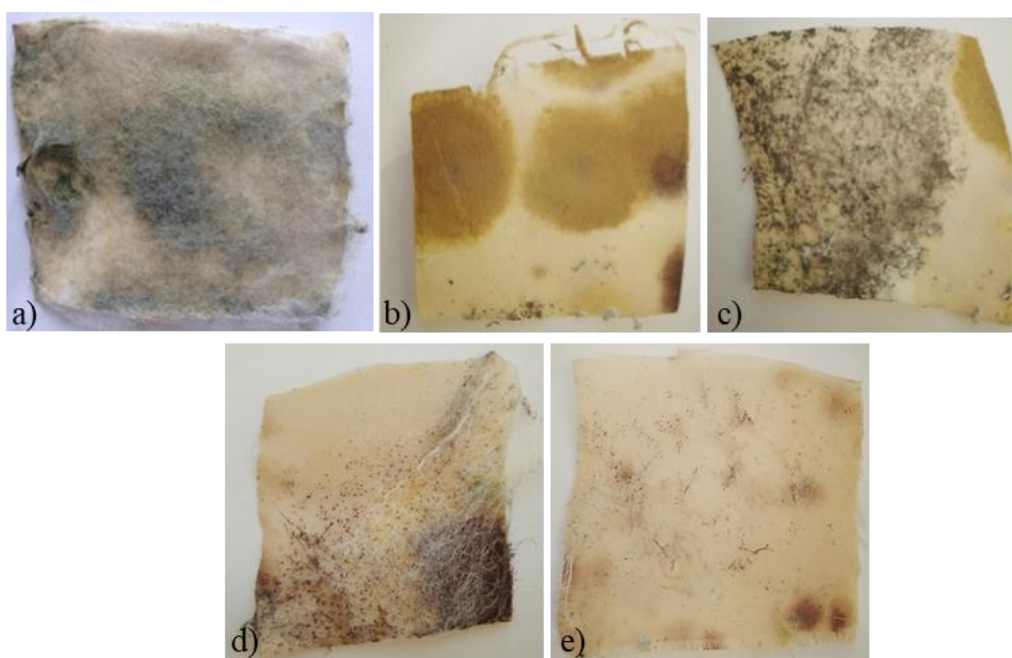
Figure 4. Photographs of samples after their exposure to microorganisms. (**a**) Uncoated silk sample, and silk samples that were coated by (**b**) Siloxane, (**c**) Siloxane+AM, (**d**) Siloxane+SiO$_2$, and (**e**) Siloxane+AM+SiO$_2$.

As shown in Figure 4a,b, the microorganisms evolve on the surface of the uncoated sample (reference silk) as well as in the silk sample coated by Siloxane. The presence of the AM agent hinders the fixation of the microorganisms onto the textile (Figure 4c). In particular, the silk sample coated by Siloxane+AM has a high number of spores (black spots) on the surface (Figure 4c) while the microorganism colonies can be clearly seen in the silk sample coated by Siloxane (Figure 4b). The use of SiO$_2$ nanoparticles enforces the response of the protective coatings against the microorganism attack. The photograph of Figure 4d shows that the presence of spores is evident on the silk, coated by Siloxane+SiO$_2$ and the microorganism colonies are not developed. Interestingly, the antimicrobial behavior of the silk sample coated by Siloxane+SiO$_2$ (Figure 4d) is comparable to the silk treated with Siloxane+AM (Figure 4c). This is explained by the superhydrophobic character of the Siloxane+SiO$_2$ coating. It should be expected that superhydrophobicity decreases adhesion and fixation of the microorganisms onto the treated silk. The response of the protective coating to microorganism attack is further enhanced when the AM is added to the Siloxane+SiO$_2$ composition (Figure 4e). According to the photograph of Figure 4e, the silk sample coated by Siloxane+AM+SiO$_2$ shows the greatest resistance to microbial attack, compared to the silk samples treated with any of the other three coatings (Figure 4b–d). The sample of Figure 4e exhibits a small number of microorganism sites and a significantly small number of spores.

In a Supplementary File, an attempt is carried out to provide some semi-quantitative data regarding the degree of contamination, which occurred in the coated samples of Figure 4. The semi-quantitative results are in agreement with the qualitative observations and conclusions which were reached using the photographs of Figure 4.

3.4. Other Evaluation Tests

The results for the vapor permeability measurements are summarized in Table 2. The weight losses per unit area (ΔW) of the vessels, which were filled with water, were measured for five consecutive days. Vessels were sealed with coated silk samples. For comparison, the corresponding measurements for

uncoated silk are included in Table 2. Using the ΔW data the relative reduction of vapor permeability (%RVP) was calculated as follows:

$$\%RVP = \left(\frac{\Delta W_u - \Delta W_c}{\Delta W_u} \right) \times 100 \tag{1}$$

where ΔW_u and ΔW_c are the weight losses of the vessels sealed by uncoated and coated silk specimens, respectively. Apparently, an ideal coating should have no effect on the water vapor permeability (%RVP = 0).

Table 2. Results of the vapor permeability tests. Weight losses (ΔW) of the vessels were measured for five consecutive days, and the %RVPs were calculated using Equation (1).

Coating on Silk	Treatment Time				
	24 h	**48 h**	**72 h**	**96 h**	**120 h**
	ΔW (g/cm^2)				
Uncoated silk (reference)	0.312	0.304	0.297	0.281	0.285
Siloxane+AM	0.198	0.198	0.202	0.201	0.201
Siloxane+SiO$_2$	0.230	0.229	0.232	0.190	0.212
Siloxane+AM+SiO$_2$	0.216	0.193	0.199	0.205	0.206
	%RVP				
Siloxane+AM	36.5	34.9	32.0	28.5	29.5
Siloxane+SiO$_2$	26.3	24.7	21.9	32.4	25.6
Siloxane+AM+SiO$_2$	30.8	36.5	33.0	27.0	27.7

The results of Table 2 suggest that the three coatings, Siloxane+AM, Siloxane+SiO$_2$, and Siloxane+AM+SiO$_2$, have roughly the same effect on the vapor permeability of silk. This conclusion is reached by comparing either the measured ΔW or the calculated %RVP values for the three coated silk samples. Using the five consecutive %RVPs, the average %RVP was calculated for each of the three coated silk specimens. The results are 32.3 ± 3.4, 26.2 ± 3.9, and 31.0 ± 3.9 for silk coated by Siloxane+AM, Siloxane+SiO$_2$, and Siloxane+AM+SiO$_2$, respectively. Hence, the coating composition has practically no effect on the breathability of silk. Vapor permeability of silk is reduced by around 30% when the superhydrophobic, superoleophobic, and antimicrobial coating of Siloxane+AM+SiO$_2$ is used for silk protection. Roughly the same result was obtained for the %RVP induced by either the Siloxane+AM or the Siloxane+SiO$_2$ coating.

A common drawback of structured coatings with special wetting properties is their poor mechanical stability and durability. To evaluate the mechanical stability of the surfaces of the coated silk samples, they were subjected to abrasion testing, and afterward, the CA of water and oil drops were measured. The results are summarized in Table 3.

Table 3. Contact angle (CA) measurements (°) of water and oil drops on four coatings on silk which were subjected to the abrasion resistance test.

Drop	CA (°) on Coated Silk			
	Siloxane	**Siloxane+AM**	**Siloxane+SiO$_2$**	**Siloxane+AM+SiO$_2$**
Water	152.0 ± 3.3	144.3 ± 2.3	163.8 ± 3.1	153.1 ± 3.3
Oil	135.3 ± 4.2	144.6 ± 4.4	144.0 ± 5.6	145.1 ± 7.8

Abrasion did not have any effect on the CA of water drops. The corresponding CA of water drops reported in Table 3 (after abrasion) and Table 1 (prior to any mechanical wear) have roughly the same values. Consequently, the superhydrophobic character of the Siloxane+SiO$_2$ and Siloxane+AM+SiO$_2$

coatings is maintained after abrasion, as the corresponding CAs remain > 150° according to the results of Table 3.

Likewise, the results in Tables 1 and 3 suggest that no major differences are observed between the corresponding CA of oil drops on silk coated by Siloxane, Siloxane+AM, and Siloxane+SiO$_2$. Abrasion had practically a noticeable effect only on the CA of oil drops on Siloxane+AM+SiO$_2$. In this case, CA drops from 157.0° (Table 1) to 145.1° (Table 3). As shown in Figure 2 the silk sample that was coated by Siloxane+AM+SiO$_2$ exhibits the highest roughness compared to the other three treated silk specimens. Consequently, the complex Siloxane+AM+SiO$_2$ coating should be the most delicate to any mechanical wear. The surface of silk coated by Siloxane+AM+SiO$_2$ after abrasion is shown in the SEM image of Figure 5. The mechanical test had a considerable effect on the surface morphology of the multifunctional coating, as revealed by comparing the SEM images of Figure 5 (after abrasion) and Figure 2d (prior to any mechanical wear). The surface structure in Figure 5 was degraded compared to that of fresh sample (Figure 2d) as some fibers and coating microclusters were damaged and rearranged because of mechanical wear. The surface tension of oil (=32 mN/m) is much lower than that of water (=72 mN/m). Hence, oil drops are more sensitive in surface structure changes. The change induced by abrasion was large enough to affect the CA of the oil drops but had no impact on the shape of water drops. This result is reported by comparing the CA values of water and oil drops on Siloxane+AM+SiO$_2$ in Tables 1 and 3.
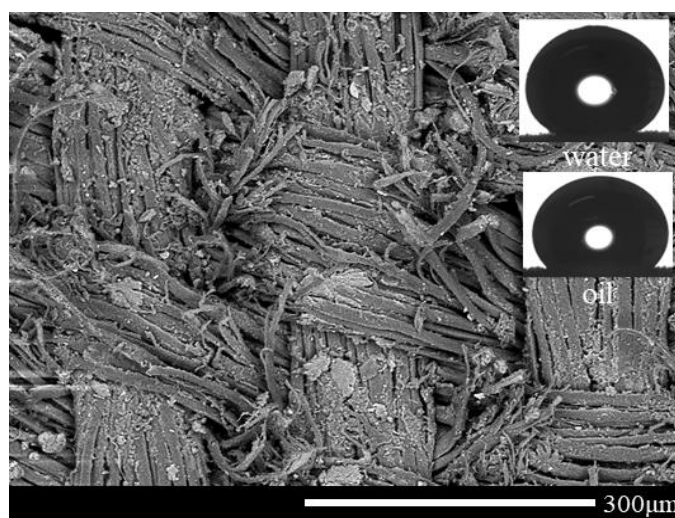
Figure 5. SEM image of silk coated by Siloxane+AM+SiO$_2$ after abrasion. Photographs of water and oil drops on the coated silk sample are included.

Overall, the results of Table 3 suggest that the multifunctional Siloxane+AM+SiO$_2$ coating shows very good mechanical stability, as after abrasion superhydrophobicity is fully maintained, whereas the coating exhibits enhanced oleophobicity, as demonstrated in Figure 5 and reported in Table 3.

Finally, the produced multifunctional Siloxane+AM+SiO$_2$ coating was evaluated through colorimetric measurements. In several applications, protective coatings should have a minimum effect on the aesthetic appearance of the underlying textile substrate. Colorimetric measurements were carried out on both uncoated silk and silk coated by Siloxane+AM+SiO$_2$. The global color difference (ΔE^*) imposed by the coating application was calculated according to Equation (2).

$$\Delta* = \sqrt{\Delta L*^2 + \Delta a*^2 + \Delta b*^2} \tag{2}$$

where *L**, *a**, and *b** are the brightness, the red–green component, and the yellow–blue component, respectively. The color change Δ*E** induced in the silk upon coating application was 2.08 ± 0.61. This is a moderate effect on the aesthetic appearance of silk which is hardly perceived by the human eye.

4. Conclusions

Superhydrophobic, superoleophobic, and antimicrobial properties were induced in silk which was sprayed and coated with an aqueous dispersion that contained alkoxy silanes, organic fluoropolymer, silane quaternary ammonium salt, and silica nanoparticles.

The extreme wetting properties were evidenced by the high contact angles (>150°) of water and oil drops on the coated silk. The deposited coating exhibits an augmented roughness raised by surface structures at the micro/nano-meter scale. Silica nanoparticles are responsible for the elevated roughness and the extreme wetting properties. The resistance of treated silk against microorganism attack is raised by the antimicrobial agent and is highly promoted by the superhydrophobic character of the coating.

The multifunctional coating induces a moderate reduction in the vapor permeability (~30%) of the treated silk, shows very good durability against abrasion, and has a minor visual effect on the aesthetic appearance of silk (Δ*E** ~2). Other evaluation tests, such as for instance the durability of the protective coating against degradation effects raised by ageing, should be carried out in a future work.

Based on the results reported herein, the suggested method has the potential to be used for the production of multifunctional coatings for the textile industry and, in principle, for the protection and preservation of textiles of the cultural heritage.

Supplementary Materials: The following are available online at http://www.mdpi.com/2079-6412/8/3/101/s1, Figure S1: Mapping of samples after their exposure to microorganisms. Contaminated areas correspond to blue-green-yellow regions and areas free of contamination are designated by red regions. Silk samples were coated by (**a**) Siloxane, (**b**) Siloxane+AM, (**c**) Siloxane+SiO_2 and (**d**) Siloxane+AM+SiO_2. The % relative contaminated areas are measured as follows: (**a**) 44.0%, (**b**) 28.4%, (**c**) 30.2% and (**d**) 6.9%; Figure S2: Absorption curves measured for potato dextrose agars (culture media). Agars were used for microorganism development on three samples coated by Siloxane+AM, Siloxane+SiO_2 and Siloxane+AM+SiO_2. For comparison, the absorption curve of agar in which no silk sample was immersed is included (reference sample).

Author Contributions: Ioannis Karapanagiotis conceived and designed the experiments; Dimitra Aslanidou performed the experiments and analyzed the data. Both authors contributed to the interpretation of the results and to the writing of the article.

Conflicts of Interest: The authors declare no conflict of interest.

References

1. Rana, M.; Hao, B.; Mu, L.; Chen, L.; Ma, P.C. Development of multi-functional cotton fabrics with Ag/AgBr-TiO_2. *Compos. Sci. Technol.* **2016**, *122*, 104–112. [CrossRef]
2. Fang, F.; Xiao, D.; Zhang, X.; Meng, Y.; Cheng, C.; Bao, C.; Ding, X.; Cao, H.; Tian, X. Construction of intumescent flame retardant and antimicrobial coating on cotton fabric via layer-by-layer assembly technology. *Surf. Coat. Technol.* **2015**, *276*, 726–734. [CrossRef]
3. Barthlott, W.; Neinhuis, C. Purity of the sacred lotus, or escape from contamination in biological surfaces. *Planta* **1997**, *202*, 1–8. [CrossRef]
4. Celia, E.; Darmanin, T.; Taffin de Givenchy, E.; Amigoni, S.; Guittard, F. Recent advances in designing superhydrophobic surfaces. *J. Colloid Interface Sci.* **2013**, *402*, 1–18. [CrossRef] [PubMed]
5. Lai, Y.K.; Chen, Z.; Lin, C.L. Recent Progress on the superhydrophobic surfaces with special adhesion: From natural to biomimetic to functional. *J. Nanoeng. Nanomanuf.* **2011**, *1*, 18–34. [CrossRef]
6. Eadie, L.; Ghosh, T.K. Biomimicry in textiles: Past, present and potential. An overview. *J. R. Soc. Interface* **2011**, *8*, 761–775. [CrossRef] [PubMed]
7. Latthe, S.S.; Gurav, A.B.; Maruti, C.S.; Vhatkar, R.S. Recent progress in preparation of superhydrophobic surfaces: A review. *J. Surf. Eng. Mater. Adv. Technol.* **2012**, *2*, 76–94.
8. Karapanagiotis, I.; Manoudis, P.N. Superhydrophobic surfaces. *JMBM* **2012**, *21*, 21–32.

9.　Samaha, M.A.; Tafreshi, H.V.; Gad-el-Hak, M. Superhydrophobic surfaces: From the lotus leaf to the submarine. *C. R. Mecanique* **2012**, *340*, 18–34. [CrossRef]

10.　Zhang, P.; Lv, F.Y. A review of the recent advances in superhydrophobic surfaces and the emerging energy-related applications. *Energy* **2015**, *82*, 1068–1087. [CrossRef]

11.　Mohamed, A.M.A.; Abdullah, A.M.; Younan, N.A. Corrosion behavior of superhydrophobic surfaces: A review. *Arab. J. Chem.* **2015**, *8*, 749–765. [CrossRef]

12.　Zhang, M.; Feng, S.; Wang, L.; Zheng, Y. Lotus effect in wetting and self-cleaning. *Biotribology* **2016**, *5*, 31–43. [CrossRef]

13.　Manoudis, P.N.; Karapanagiotis, I. Modification of the wettability of polymer surfaces using nanoparticles. *Prog. Org. Coat.* **2014**, *77*, 331–338. [CrossRef]

14.　Bhushan, B.; Koch, K.; Jung, Y.C. Fabrication and characterization of the hierarchical structure for superhydrophobicity and self-cleaning. *Ultramicroscopy* **2009**, *109*, 1029–1034. [CrossRef] [PubMed]

15.　Bernagozzi, I.; Torrengo, S.; Minati, L.; Ferrari, M.; Chiappini, A.; Armellini, C.; Toniutti, L.; Lunelli, L.; Speranza, G. Synthesis and characterization of PMMA based superhydrophobic surfaces. *Colloid Polym. Sci.* **2012**, *290*, 315–322. [CrossRef]

16.　Lakshmi, R.V.; Bharathidasan, T.; Basu, B.J. Superhydrophobic sol–gel nanocomposite coatings with enhanced hardness. *Appl. Surf. Sci.* **2011**, *257*, 10421–10426. [CrossRef]

17.　Karapanagiotis, I.; Pavlou, A.; Manoudis, P.N.; Aifantis, K.E. Water repellent ORMOSIL films for the protection of stone and other materials. *Mater. Lett.* **2014**, *131*, 276–279. [CrossRef]

18.　Wang, T.; Isimjan, T.T.; Chen, J.; Rohani, S. Transparent nanostructured coatings with UV-shielding and superhydrophobicity properties. *Nanotechnology* **2011**, *22*, 265708. [CrossRef] [PubMed]

19.　Li, Y.; Zhang, Z.; Zhu, X.; Men, X.; Ge, B.; Zhou, X. Fabrication of a superhydrophobic coating with high adhesive effect to substrates and tunable wettability. *Appl. Surf. Sci.* **2015**, *328*, 475–481. [CrossRef]

20.　Barshilia, H.C.; Gupta, N. Superhydrophobic polytetrafluoroethylene surfaces with leaf-like micro-protrusions through Ar + O_2 plasma etching process. *Vacuum* **2014**, *99*, 42–48. [CrossRef]

21.　Karapanagiotis, I.; Grosu, D.; Aslanidou, D.; Aifantis, K.E. Facile method to prepare superhydrophobic and water repellent cellulosic paper. *J. Nanomater.* **2015**, *16*, 11. [CrossRef]

22.　Chatzigrigoriou, A.; Manoudis, P.N.; Karapanagiotis, I. Fabrication of water repellent coatings using waterborne resins for the protection of the cultural heritage. *Macromol. Symp.* **2013**, *331*, 158–165. [CrossRef]

23.　Karapanagiotis, I.; Manoudis, P.N.; Savva, A.; Panayiotou, C. Superhydrophobic polymer-particle composite films produced using various particle sizes. *Surf. Interface Anal.* **2012**, *44*, 870–875. [CrossRef]

24.　Manoudis, P.N.; Karapanagiotis, I.; Tsakalof, A.; Zuburtikudis, I.; Kolinkeová, B.; Panayiotou, C. Superhydrophobic films for the protection of outdoor cultural heritage assets. *Appl. Phys. A Mater.* **2009**, *97*, 351–360. [CrossRef]

25.　Ovaskainena, L.; Rodriguez-Meizoso, I.; Birkin, N.A.; Howdle, S.M.; Gedde, U.; Wågberg, L.; Turner, C. Towards superhydrophobic coatings made by non-fluorinated polymers sprayed from a supercritical solution. *J. Supercrit. Fluids* **2013**, *77*, 134–141. [CrossRef]

26.　Quana, C.; Werner, O.; Wågberg, L.; Turner, C. Generation of superhydrophobic paper surfaces by a rapidly expanding alkyl ketene dimer—Supercritical carbon dioxide solution. *J. Supercrit. Fluids* **2009**, *49*, 117–124. [CrossRef]

27.　Cao, L.; Price, T.P.; Weiss, M.; Gao, D. Super water- and oil-repellent surfaces on intrinsically hydrophilic and oleophilic porous silicon films. *Langmuir* **2008**, *24*, 1640–1643. [CrossRef] [PubMed]

28.　Tuteja, A.; Choi, W.; Mabry, J.M.; McKinley, G.H.; Cohen, R.E. Robust omniphobic surfaces. *Proc. Natl. Acad. Sci. USA* **2008**, *105*, 18200–18205. [CrossRef] [PubMed]

29.　Choi, W.; Tuteja, A.; Chhatre, S.; Mabry, J.M.; Cohen, R.E.; McKinley, G.H. Fabrics with tunable oleophobicity. *Adv. Mater.* **2009**, *21*, 2190–2195. [CrossRef]

30.　Kota, A.K.; Li, Y.; Mabry, J.M.; Tuteja, A. Hierarchically structured superoleophobic surfaces with ultralow contact angle hysteresis. *Adv. Mater.* **2012**, *24*, 5838–5843. [CrossRef] [PubMed]

31.　Kim, P.; Wong, T.-S.; Alvarenga, J.; Kreder, M.J.; Adorno-Martinez, W.E.; Aizenberg, J. Liquid-infused nanostructured surfaces with extreme anti-ice and anti-frost performance. *ACS Nano* **2012**, *6*, 6569–6577. [CrossRef] [PubMed]

32.　Lafuma, A.; Quéré, D. Slippery pre-suffused surfaces. *Europhys. Lett.* **2011**, *96*, 56001. [CrossRef]

33.　Wong, T.S.; Kang, S.H.; Tang, S.K.Y.; Smythe, E.J.; Hatton, B.D.; Grinthal, A.; Aizenberg, J. Bioinspired self-repairing slippery surfaces with pressure-stable omniphobicity. *Nature* **2011**, *477*, 443–447. [CrossRef] [PubMed]

34.　Richard, D.; Quéré, D. Bouncing water drops. *Europhys. Lett.* **2000**, *50*, 769–775. [CrossRef]

35.　Wu, Y.; Su, B.; Jiang, L.; Heeger, A.J. "Liquid-liquid-solid"-type superoleophobic surfaces to pattern polymeric semiconductors towards high-quality organic field-effect transistors. *Adv. Mater.* **2013**, *25*, 6526–6533. [CrossRef] [PubMed]

36.　Bormashenko, E.; Grynyov, R.; Chaniel, G.; Taitelbaum, H.; Bormashenko, Y. Robust technique allowing manufacturing superoleophobic surfaces. *Appl. Surf. Sci.* **2013**, *270*, 98–103. [CrossRef]

37.　Pechook, S.; Kornblum, N.; Pokroy, B. Bio-inspired superoleophobic fluorinated wax crystalline surfaces. *Adv. Funct. Mater.* **2013**, *23*, 4572–4576. [CrossRef]

38.　Fujii, T.; Aoki, Y.; Habazaki, H. Fabrication of super-oil-repellent dual pillar surfaces with optimized oillar intervals. *Langmuir* **2011**, *27*, 11752–11756. [CrossRef] [PubMed]

39.　Darmanin, T.; Guittard, F.; Amigoni, S.; de Givenchy, E.T.; Noblin, X.; Kofman, R.; Celestini, F. Superoleophobic behavior of fluorinated conductive polymer films combining electropolymerization and lithography. *Soft Matter* **2011**, *7*, 1053–1057. [CrossRef]

40.　Steele, A.; Bayer, I.; Loth, E. Inherently superoleophobic nanocomposite coatings by spray atomization. *Nano Lett.* **2009**, *9*, 501–505. [CrossRef] [PubMed]

41.　Sheen, Y.C.; Chang, W.H.; Chen, W.C.; Chang, Y.H.; Huang, Y.C.; Chang, F.C. Non-fluorinated superamphiphobic surfaces through sol–gel processing of methyltriethoxysilane and tetraethoxysilane. *Mater. Chem. Phys.* **2009**, *114*, 63–68. [CrossRef]

42.　Hoefnagels, H.F.; Wu, D.; de With, G.; Ming, W. Biomimetic superhydrophobic and highly oleophobic cotton textiles. *Langmuir* **2007**, *23*, 13158–13163. [CrossRef] [PubMed]

43.　Artusa, G.R.J.; Zimmermann, J.; Reifler, F.A.; Brewer, S.A.; Seeger, S.A. Superoleophobic textile repellent towards impacting drops of alkanes. *Appl. Surf. Sci.* **2012**, *258*, 3835–3840. [CrossRef]

44.　Leng, B.X.; Shao, Z.Z.; de With, G.; Ming, W.H. Superoleophobic cotton textiles. *Langmuir* **2009**, *25*, 2456–2460. [CrossRef] [PubMed]

45.　Liu, F.; Ma, M.; Zang, D.; Gao, Z.; Wang, C. Fabrication of superhydrophobic/superoleophilic cotton for application in the field of water/oil separation. *Carbohydr. Polym.* **2014**, *103*, 480–487. [CrossRef] [PubMed]

46.　Zhang, M.; Wang, S.; Wang, C.; Li, J. A facile method to fabricate superhydrophobic cotton fabrics. *Appl. Surf. Sci.* **2012**, *261*, 561–566. [CrossRef]

47.　Wang, H.; Xue, Y.; Lin, T. One-step vapour-phase formation of patternable, electrically conductive, superamphiphobic coatings on fibrous materials. *Soft Matter* **2011**, *7*, 8158–8161. [CrossRef]

48.　Zhou, X.; Zhang, Z.; Xu, X.; Men, X.; Zhu, X. Fabrication of super-repellent cotton textiles with rapid reversible wettability switching of diverse liquid. *Appl. Surf. Sci.* **2013**, *276*, 571–577. [CrossRef]

49.　Saraf, R.; Lee, H.J.; Michielsen, S.; Owens, J.; Willis, C.; Stone, C.; Wilusz, E. Comparison of three methods for generating superhydrophobic, superoleophobic nylon nonwoven surface. *J. Mater. Sci.* **2011**, *46*, 5751–5760. [CrossRef]

50.　Hayn, R.A.; Owens, J.R.; Boyer, S.A.; McDonald, R.S.; Lee, H.J. Preparation of highly hydrophobic and oleophobic textile surfaces using microwave-promoted silane coupling. *J. Mater. Sci.* **2011**, *46*, 2503–2509. [CrossRef]

51.　Shirgholami, M.A.; Khalil-Abad, M.S.; Khajavi, R.; Yazdanshenas, M.E. Fabrication of superhydrophobic polymethylsilsesquioxane nanostructures on cotton textiles by a solution immersion process. *J. Colloid Interface Sci.* **2011**, *359*, 530–535. [CrossRef] [PubMed]

52.　Sataev, M.S.; Koshkarbaeva, S.T.; Tleuova, A.B.; Perni, S.; Aidarova, S.B.; Prokopovich, P. Novel process for coating textile materials with silver to prepare antimicrobial fabrics. *Colloids Surfaces A* **2014**, *442*, 146–151. [CrossRef]

53.　Hassan, M.M. Antimicrobial coatings for textiles. In *Handbook of Antimicrobial Coatings*; Atul, T., Ed.; Elsevier Inc.: Amsterdam, The Netherlands, 2018; pp. 321–355.

54.　Coradia, M.; Zanettia, M.; Valério, A.; de Oliveira, D.; da Silva, O.; de Arruda, S.M.; de Souza, G.U.; de Souza, A.A.U. Production of antimicrobial textiles by cotton fabric functionalization and pectinolytic enzyme immobilization. *Mater. Chem. Phys.* **2018**, *208*, 28–34. [CrossRef]

55. Terzioglu, F.; Grethe, T.; Both, C.; Joßen, A.; Mahltig, B.; Rabe, M. Coating technologies for antimicrobial textile surfaces: State of the art and future prospects for textile finishing. In *Handbook of Antimicrobial Coatings*; Elsevier Inc.: Amsterdam, The Netherlands, 2018; pp. 123–135.

56. Ulaeto, S.B.; Rajan, R.; Pancrecious, J.K.; Rajan, T.P.D.; Pai, B.C. Developments in smart anticorrosive coatings with multifunctional characteristics. *Prog. Org. Coat.* **2017**, *111*, 294–314. [CrossRef]

57. Pospiech, D.; Jehnichen, D.; Stark, S.; Müller, F.; Bünker, T.; Wollenberg, A.; Häußler, L.; Simone, F.; Grundke, K.; Oertel, U.; et al. Multifunctional methacrylate-based coatings for glass and metal. *Appl. Surf. Sci.* **2017**, *399*, 205–214. [CrossRef]

58. Colangiuli, D.; Calia, A.; Bianco, N. Novel multifunctional coatings with photocatalytic and hydrophobic properties for the preservation of the stone building heritage. *Constr. Build. Mater.* **2015**, *93*, 189–196. [CrossRef]

59. Zarzuela, R.; Carbú, M.; Gil, M.L.A.; Cantoral, J.M.; Mosquera, M.J. CuO/SiO_2 nanocomposites: A multifunctional coating for application on building stone. *Mater. Des.* **2017**, *114*, 364–372. [CrossRef]

60. Goffredo, G.B.; Terlizzi, V.; Munafò, P. Multifunctional TiO_2-based hybrid coatings on limestone: Initial performances and durability over time. *J. Build. Eng.* **2017**, *14*, 134–149. [CrossRef]

61. La Russa, M.F.; Ruffolo, S.A.; Rovella, N.; Belfiore, C.M.; Palermo, A.M.; Guzzi, M.T.; Crisci, G.M. Multifuntional TiO_2 coatings for cultural heritage. *Prog. Org. Coat.* **2012**, *74*, 186–191. [CrossRef]

62. Attia, N.F.; Moussa, M.; Sheta, A.M.F.; Taha, R.; Gamal, H. Synthesis of effective multifunctional textile based on silica nanoparticlesOriginal. *Prog. Org. Coat.* **2017**, *106*, 41–49. [CrossRef]

63. Aranzabe, E.; Arriortua, M.I.; Larrañaga, A.; Aranzabe, A.; Villasante, P.M.; March, R. Designing multifunctional pigments for an improved energy efficiency in buildings. *Energy Build.* **2017**, *147*, 9–13. [CrossRef]

64. Fox-Rabinovich, G.S.; Beake, B.D.; Yamamoto, K.; Aguirre, M.H.; Veldhuis, S.C.; Dosbaeva, G.; Elfizy, A.; Biksa, A.; Shuster, L.S. Structure, properties and wear performance of nano-multilayered. TiAlCrSiYN/ TiAlCrN coatings during machining of Ni-based aerospace superalloys. *Surf. Coat. Technol.* **2010**, *204*, 3698–3706. [CrossRef]

65. Cannavale, A.; Fiorito, F.; Manca, M.; Tortorici, G.; Cingolani, R.; Gigli, G. Multifunctional bioinspired sol-gel coatings for architectural glasses. *Build. Environ.* **2010**, *45*, 1233–1243. [CrossRef]

66. Aslanidou, D.; Karapanagiotis, I.; Panayiotou, C. Superhydrophobic, superoleophobic coatings for the protection of silk textiles. *Prog. Org. Coat.* **2016**, *97*, 44–52. [CrossRef]

67. Aslanidou, D.; Karapanagiotis, I.; Panayiotou, C. Tuneable textile cleaning and disinfection process based on supercritical CO_2 and Pickering emulsions. *J. Supercrit. Fluids* **2016**, *118*, 128–139. [CrossRef]

68. Jain, A.; Duvvuri, L.S.; Farah, S.; Beyth, N.; Domb, A.J.; Khan, W. Antimicrobial polymers. *Adv. Healthc. Mater.* **2014**, *3*, 1969–1985. [CrossRef] [PubMed]

69. Rozman, U.; Zavec Pavlinić, D.; Pal, E.; Gönc, V.; Šostar Turk, Z. *Efficiency of Medical Workers' Uniforms with Antimicrobial Textiles for Advanced Applications*; Kumar, B., Thakur, S., Eds.; InTech: Rijeka, Croatia, 2017.

70. Jiao, Y.; Niu, L.; Ma, S.; Li, J.; Tay, F.R.; Chen, J. Quaternary ammonium-based biomedical materials: State-of-the-art, toxicological aspects and antimicrobial resistance. *Prog. Polym. Sci.* **2017**, *71*, 53–90. [CrossRef]

71. Yao, C.; Li, X.; Neoh, K.G.; Shi, Z.; Kang, E.T. Surface modification and antibacterial activity of electrospun polyurethane fibrous membranes with quaternary ammonium moieties. *J. Membr. Sci.* **2008**, *320*, 259–267. [CrossRef]

72. Wessels, S.; Ingmer, H. Modes of action of three disinfectant active substances: A review. *Regul. Toxicol. Pharmacol.* **2013**, *67*, 456–467. [CrossRef] [PubMed]